

Synthesis and fabrication of MnFe_2O_4 spinel ferrite thin films using chemical approach: Structural, magnetic, optical and magneto-optical properties

Ramakanth Illa^{*1,2}, Jaroslav Hamrle^{1,3,4}, Jaromir Pištora^{1,3}

¹Nanotechnology Centre, VŠB - Technical University of Ostrava, 17. listopadu 15, Ostrava - Poruba, 70833, Czech Republic

²Department of Chemistry, Rajiv Gandhi University of Knowledge Technologies, IIIT-Nuzvid, Andhra Pradesh 521202, India

³Department of Physics, VŠB - Technical University of Ostrava, 17. listopadu 15, Ostrava - Poruba, 70833, Czech Republic

⁴Faculty of Mathematics and Physics, Charles University, Ke Karlovu 3, Prague, 12116, Czech Republic

*Corresponding author, E-mail: ramakanthilla@yahoo.com; Tel: (+42) 0-597329356

Received: 07 April 2016, Revised: 27 September 2016 and Accepted: 20 December 2016

DOI: 10.5185/amp.2017/3013

www.vbripress.com/amp

Abstract

Nanostructured thin films of MnFe_2O_4 were fabricated using chemical approach. Structural, magnetic, optical and magneto-optical properties of the films have been investigated using XRD, AFM, VSM, spectroscopic ellipsometry and MOKE spectroscopy. Structural evaluation of the thermally annealed films showed crystalline phase and spinel structure along with appearance of textured nano-crystallites at the annealing temperature (T_a) of 500 °C and above. Surface morphology of the films annealed at 600 °C was characterized using AFM and the size of MnFe_2O_4 particles was observed to be 70 – 180 nm with ellipsoidal morphology and the surface roughness was found to be 8 nm. Hysteresis loops of the ferrite films indicated ferromagnetic behavior for annealing temperature of 400 °C and above, with a small contribution of paramagnetic nature arising from its oxide. The films showed a semiconducting behavior for the annealing temperature (T_a) ranging from 400 - 600 °C. The magneto-optical response is found to be small, *i.e.*, one order less when compared to CoFe_2O_4 or metallic Fe, Co films. The maximum magneto-optical response from MnFe_2O_4 thin films is found for $T_a = 400$ °C, *i.e.* for incomplete spinel structure. As the material used for making the thin film coating is of the order of very few milligrams, these highly responsive films could be used as magnetic sensors. Copyright © 2017 VBRI Press.

Keywords: Manganese ferrite, thin films, physical properties, magneto-optical properties, MOKE.

Introduction

New magnetic materials have attracted much attention due to the integral role they play in magnetic sensing [1] and high-density data storage [2, 3]. Among various magnetic materials, ferrites have interesting magneto-optical applications due to their unique physical properties. Nanosized room temperature ferromagnets are used for memory applications *i.e.* materials with high magnetization and switchability that contribute to thin film architectures for device development. Due to the excellent electrical and magnetic properties, high magnetic permeability and electrical resistance, spinel ferrites are used in the field of microwave, and electronic devices [4]. Even though extensive research has been done on ferrite materials, exploring

new ways of synthetic routes and improving physical properties is still interesting to extend their applications [5, 6].

As the crystallite size has large influence on magnetic properties of the material, thin films of ferrites have potential interest in magneto-optical applications [7]. For investigations using the optical and magneto-optical effect, the thin films must be homogeneous, continuous and transparent. Ferrite films are optically transparent up to a film thickness of typically 1 μm , depending on the cation ratio. An important requirement for magneto-optical applications (Faraday and Kerr effect) is that the films must be very smooth. High quality ferrite thin films are useful for most of the magnetic devices that require low magnetic losses and tailored magnetic properties [8].

Due to the difference in properties of the magnetic nanoparticles from their bulk counterparts, the magnetic nanoparticles approach the superparamagnetic limit where ambient thermal energy can randomize the magnetization leading to nanomaterials with zero coercivity and zero remanent magnetization [9]. Designing nanomagnets which can retain high magnetization, non-zero coercivity, and remanence is of technological importance which requires weak ferromagnetism. While developing magnetic data storage devices, the ability to reduce a bulk magnetic material to the nanoscale without affecting its innate ferromagnetic character is of great importance. Several methods to form thin films of magnetic nanomaterials have been reported in literature via electrodeposition [5], sol-gel techniques [10] and pulsed-laser deposition (PLD) [11]. Nanorods [12, 13], nanocrystals [14-16], ordered nanocrystal arrays [17] and nanocrystal superlattices [18] were also grown from magnetic materials using various preparation routes. Transition metal oxides such as the ferrites are particularly useful as they combine interesting magnetic and electrical properties with stability against oxidation. Thus, ferrites constitute an important class of materials that are used extensively in the field of magnetic memory [19].

Soft magnetic thin films with high electrical resistivity to develop microinductors and microtransformers have been reported [20]. The development of ferrite films for use in monolithic microwave integrated circuits is an area of active research [21]. Magnetic properties of ferrite films are more sensitive to crystalline disorder than those of metal films, such as permalloy. Soft magnetic thin films of Cobalt ferrite are used as high magnetostrictive material for stress, pressure and torsion sensors, catalysts or gas/humidity sensors [22] and micro actuators [23]. Ferrite based microwave tunable devices which include phase shifters and filters permit the control of microwave properties by application of stationary or time varying magnetic field. Similar to MEMS capacitors, ferrite devices can be tuned continuously or switched between two states. Unlike magnetic metal, ferrite is a magnetic dielectric that allows an electromagnetic wave to penetrate through itself, thereby initiating an interaction between the wave and the magnetization within ferrite. This interaction has been used to produce a plethora of useful devices [24].

New tunable technologies are being developed that can show excellent performance with smaller size and lower power consumptions. In most cases, fabrication that is attuned with high levels of integration. These also include the thin films of ferrite or ferromagnetic composite devices [25]. The progress on miniaturization and integration of microwave devices strongly depends on the ability to fabricate high quality tunable thin films possessing for both high tunability and low loss. Among the soft magnetic ferrite materials, MnFe_2O_4 is important due

to its applications in the gas sensors, absorbent material for hot gases and also as a potential candidate of contrast agents in magnetic resonance imaging (MRI). The superparamagnetic MnFe_2O_4 nanoparticles were found to have a very high magnetization and large relaxivity owing to their large magnetic spin magnitude [26, 27]. The preparation condition – property correlations of MnFe_2O_4 thin films depend on the composition, morphology and size of the particles [28]. As the magnetic properties of ferrite thin films are strongly dependent on both their nanostructures and the deposition methods, the objective of this work was to synthesize and fabricate MnFe_2O_4 thin films and to investigate their structural, magnetic, optical and magneto-optical properties. The fabricated films were subjected to XRD, AFM, VSM, ellipsometry and MOKE spectroscopy. The films were fabricated using the simple and cost effective dip coating method with an id Lab dip-coater instrument.

Several ferrite thin films have been reported in the literature in order to look at mainly the structural aspects. However, the effect of citric acid to ethylene glycol ratio and ethanol were not focused in the fabrication of thin films [29]. Therefore, the main objective of this work was to study the morphology, effect of citric acid to ethylene glycol ratio, and minimizing the quantities of precursors for fabricating highly responsive thin films of manganese ferrite as a function of various annealing temperatures. As the material used for making the thin film coating is of the order of very few milligrams on the glass substrate, these highly responsive films could be used as magnetic sensors.

Experimental

Materials

$\text{Fe}(\text{NO}_3)_3 \cdot 9\text{H}_2\text{O}$ of 99.9 % purity, $\text{MnCl}_2 \cdot 4\text{H}_2\text{O}$, Ethylene glycol (spectrophotometric grade, $\geq 99\%$) and Citric acid monohydrate (ACS reagent, $\geq 99\%$) were purchased from Sigma-Aldrich, Germany and glass substrates purchased from VWR International, U.K.

Material synthesis and fabrication of thin films

Synthesis and fabrication: Stoichiometric amounts of the metal salt precursors $\text{Fe}(\text{NO}_3)_3 \cdot 9\text{H}_2\text{O}$ (0.811 g) and $\text{MnCl}_2 \cdot 4\text{H}_2\text{O}$ (0.4947 g) were dissolved in 25 mL of ultrapure water from a Millipore Elix A3-MilliQ system (MilliQ, Germany) to get a clear yellow colored solution. Aqueous solution of citric acid (6.3 g in 100 mL) was added to the precursors solution with constant magnetic stirring for 6 hrs. The mole ratio of the precursors to citric acid ratio was maintained to be 1:4. The ratio of precursor mixture, citric acid and ethylene glycol ratio was maintained to be 1:4:5 respectively. The solution mixture was evaporated on a hot plate at 70 °C for 4 hrs. Then ethylene glycol was added at 90 °C and the solution

was slowly evaporated until a highly viscous solution was formed. Finally, an equivalent volume of ethanol was added to that of viscous sol present such that the final solution contains 1:1 mixture of viscous sol and ethanol. Films were dip-coated from the solution onto glass substrates by vertical dipping method using id LAB dip-coater instrument. The withdrawal rate maintained was 60 mm/min depending on the desired thickness. The films were dried at 200 °C for 2 h to form homogeneous, transparent and continuous thin films. The as prepared films were finally annealed at 300, 400, 500, and 600 °C, respectively.

Methods and characterization

X-ray diffraction (XRD)

X-ray diffraction patterns were recorded under CoK α irradiation ($\lambda = 1.789 \text{ \AA}$, 35 kV, 25 mA) using the Bruker D8 Advance diffractometer (Bruker AXS) equipped with a fast position sensitive detector VÅNTEC 1. Measurements were carried out in the reflection mode in Bragg-Brentano geometry. Data were collected in the 3–100° 2 θ angular range.

Atomic force microscopy (AFM)

The morphology of the surfaces, and roughness of the thin films were studied using EXPLORERTM atomic force microscopy. The annealed films were investigated with SOLVER NEXT (NT-MDT) atomic force microscope equipped with contact probe PPP-CONTR (Nanosensors) for imaging. The images were evaluated using Gwyddion software.

Vibrating sample magnetometry (VSM)

Magnetic properties of the annealed MnFe₂O₄ films were investigated using Microsense EV9 Vibration Sample Magnetometer with the maximal applied magnetic field 2 T at room temperature. Parameters obtained from measured magnetization curves (coercive field, remanent and saturation magnetization) were analysed as a function of annealing temperature.

Spectroscopic ellipsometry

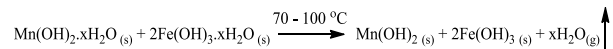
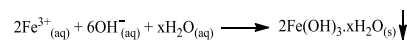
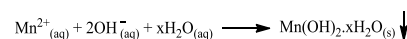
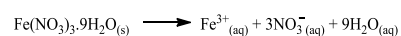
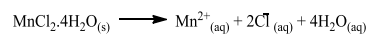
The ellipsometry investigation was done by Woollam RC2 ellipsometer measuring spectra of Mueller matrix components, in spectral range 0.8-6.4 eV. The ellipsometric data are expressed as complex pseudo-dielectric functions (ϵ_{pseudo}) having its real and imaginary parts, and providing equal data as classical ellipsometry Ψ , Δ (i.e. there is a direct transformation between ϵ_{pseudo} and Ψ , Δ). The ellipsometry data expressed by ϵ_{pseudo} corresponds to the case, when experimental ellipsometry data are expressed by optical properties of ideal effective sample consisting of homogeneous bulk material with smooth interface. The advantage of this approach is small dependence on incidence angle of the pseudo-dielectric function. Ellipsometric measurements were performed for the incidence angles from 50° to 80° with 5° step.

The experimental data were fitted by multilayer optical model. In this model, the imaginary part of the dielectric function (i.e. light absorption) is described by so called B-spline, i.e. we define absorption values for about 30 photon energies, which then determine absorption function as a spline of those points [30]. The real part of dielectric function is calculated from the imaginary one using Kramers-Kronig relation [31]. The fitting was done in Complete EASE ellipsometric software provided with the ellipsometer.

Magneto-optical Kerr effect (MOKE)

The MOKE spectra (spectra of Kerr rotation and Kerr ellipticity) were measured on home-build system in the spectral range 1.5 – 4.7 eV. The measurements were done at reflection at nearly perpendicular incidence angle (2°), at external field 0.18 T perpendicular to sample surface. The off-diagonal magneto-optical function K is determined by fit to experimental MOKE spectra using home-written multilayer model [32].

Reactions:



Results and discussion

MnFe₂O₄ is a cubic spinel with two divalent cation sites composed of 8 tetrahedral A sites and 16 octahedral B sites. The Mn²⁺ and Fe³⁺ ions have half-filled 3d shell and, as a consequence, their ground state is the singlet 6S with spin 5/2 and zero orbital momentum, which is not split by a crystal field. Mn³⁺ has the electronic configuration of 3d⁴, which in the free ion yields 5D multiplet, (both spin and orbital momentum) as the ground state [33-35]. The fabrication of nanostructured MnFe₂O₄ thin films was carried out by chemical approach using metal nitrate and chloride salts as the precursors as mentioned in the experimental section. The dip-coated MnFe₂O₄ thin films were thermally annealed at 300, 400, 500 and 600 °C.

Structural investigation using X-ray diffraction analysis

The microstructures of the thermally annealed MnFe₂O₄ thin films have been investigated using X-ray diffraction technique. The structural analysis has been carried out for MnFe₂O₄ with the thin films annealed from 300 – 600 °C. MnFe₂O₄ thin film

samples annealed from 300 – 400 °C indicated that the crystalline phase formation was incomplete. The temperature range required to decompose chloride and nitrate precursors in the thin film was found to be in between 300 – 400 °C. From **Fig. 1**, one can see that the reflection peaks become sharper and prominent on increasing the annealing temperature indicating that crystallinity tends to improve.

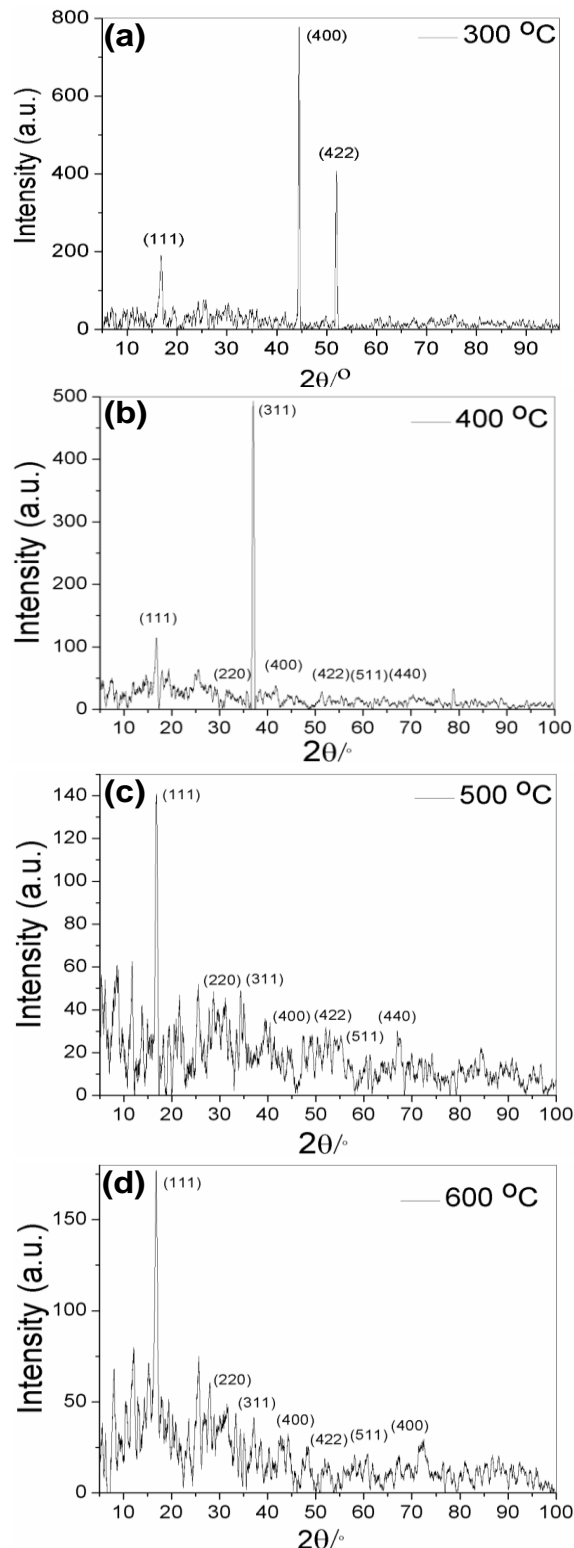


Fig. 1. Wide angle XRD spectra of the MnFe_2O_4 thin films annealed at (a) 300 °C (b) 400 °C (c) 500 °C (d) 600 °C.

It can be seen from **Fig. 1** that there are nanocrystallites with different orientations when Ta is 500 °C. These structural transitions have also been reflected by the change of both optical and magneto-optical properties. The crystallites present an ellipsoidal shape with a narrow particle size distribution. The indexed peaks are related to the spinel phase structure according to JCPDS Data Base (JCPDS no.10-0319).

Surface morphology using Atomic Force Microscopic analysis

Atomic Force Microscopy gives the nanostructural behavior of the ferrite thin films [36]. Surface morphology of the MnFe_2O_4 thin films annealed at 600 °C was characterized using AFM. **Fig. 2(a&b)** shows the AFM images of the as prepared MnFe_2O_4 films. The film consists of nanoscale MnFe_2O_4 particles of size in the range ~ 70 – 180 nm with ellipsoidal morphology and the surface roughness was found to be 8 nm.

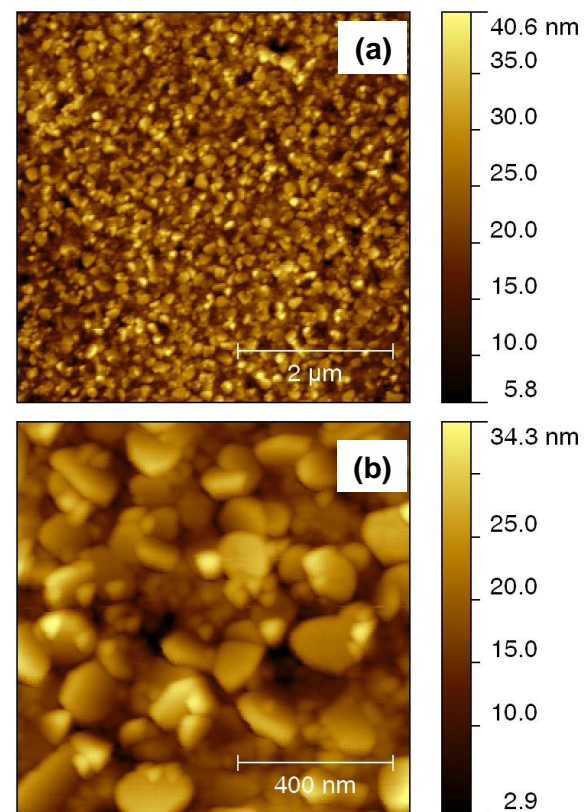


Fig. 2. (a & b) AFM images of MnFe_2O_4 films fabricated on glass substrates using chemical approach and subsequently annealed at 600 °C for 2 hrs.

Fig. 2 shows the homogeneous micro-structures of MnFe_2O_4 with nano grain size and a uniform size distribution. The surface of the thin films was observed to be crack-free and smooth. The films revealed that the crystallites exhibited ellipsoidal shape with a small grain boundary region for all the films. The average crystallite size was observed to be 125 nm for MnFe_2O_4 thin films from AFM

measurements. This average crystallite size value measured from AFM is almost consistent with the calculated value from XRD investigations. The smaller nano crystallite formation of these ferrites could be attributed to the present chemical approach of better stoichiometric ratio and low processing temperature for crystallization.

Magnetic properties of $MnFe_2O_4$ thin films using Vibrating Sample Magnetometry

The magnetic properties of $MnFe_2O_4$ thin films have been investigated using Vibrating Sample Magnetometry (VSM) at room temperature. To determine magnetic properties of $MnFe_2O_4$, the total magnetic moment of the sample was subtracted from independently measured magnetic moment of glass substrate (5x5x0.5 mm). The hysteresis loops of the measured magnetic moment of whole samples are shown in **Fig. S1** (supporting information) and **Fig. 3** (extracted volume magnetization of $MnFe_2O_4$ where $MnFe_2O_4$ thickness is estimated 30 nm from ellipsometry measurements). Hysteresis loops were recorded to determine saturation magnetization (M_s) and coercivity (H_c) given in **Table 1**.

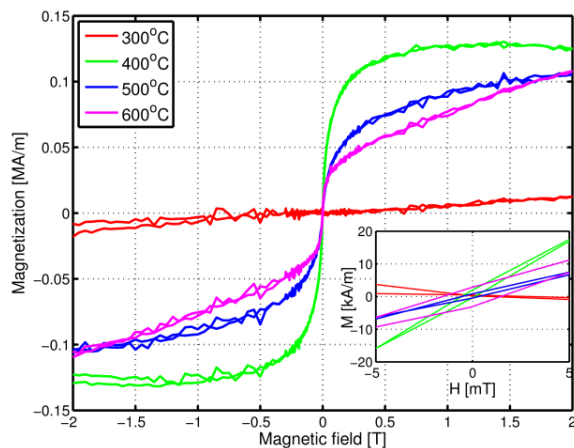


Fig. 3. M–H hysteresis loops for $MnFe_2O_4$ films (after subtracting glass contribution). The inset shows the zoomed hysteresis loops in vicinity of zero magnetic field.

For 300 °C, only linear M-H dependence is found and no saturation is found upto field 2 T. Higher annealing temperatures provide saturating hysteresis loops with very small coercive field (in order of mT - see **Table 1**).

Table 1. Magnetic parameters of $MnFe_2O_4$ films extracted from M-H hysteresis loops.

Annealing Temperature [°C]	Magnetization @ 2 T [kA/m]	Coercivity, H_c [mT]
300	12	0
400	124	0.6
500	107	0.8
600	104	2.9

The value of saturation magnetization is the largest for 400 °C, being 124 kA/m = 0.16 T, and slightly decreases for higher annealing temperature (see Tab. 1). It suggests that complete spinel structure provides smaller saturation magnetization compared to incomplete spinel structure. There is no significant difference of their magnetic properties for external fields applied parallel and perpendicular to their planes. The values of saturation magnetization are about 1/3 compared to bulk $MnFe_2O_4$, which is 80 emu/g = 80 Am²/kg. With density 5000 kg/m³ it provides volume magnetization $M = 400$ kA/m = 0.50 T [37]. Large reduction of saturation magnetization in nanoparticles is well-known, e.g. nanoparticles $MnFe_2O_4$ in Ref. [38] demonstrated mass saturation magnetization 46 Am²/kg = 46 emu/g [37]. Such behavior is ascribed to the surface effects in nanoparticles. The surface effect may be developed due to the existence of an inactive magnetic layer or a disordered layer on the surface of nanoparticles and/or the heating rate of calcination. It is well known that, as annealing temperature increases, occupation ratio of iron ions at octahedral sites decreases. Therefore, magnetic moment of ferrite nanoparticles is enhanced. Usually, the size, coercivity, and saturation magnetization of ferrite particles increases with the annealing temperature [39]. However, in our case the saturation magnetization is found maximum at 400 °C.

Optical properties of $MnFe_2O_4$ thin films: Spectroscopic Ellipsometry

The experimental ellipsometry data of $MnFe_2O_4$ are shown in **Fig. 4**, expressed in the form of pseudo-dielectric function. In order to determine the dielectric constant of $MnFe_2O_4$, the optical multilayer model is employed.

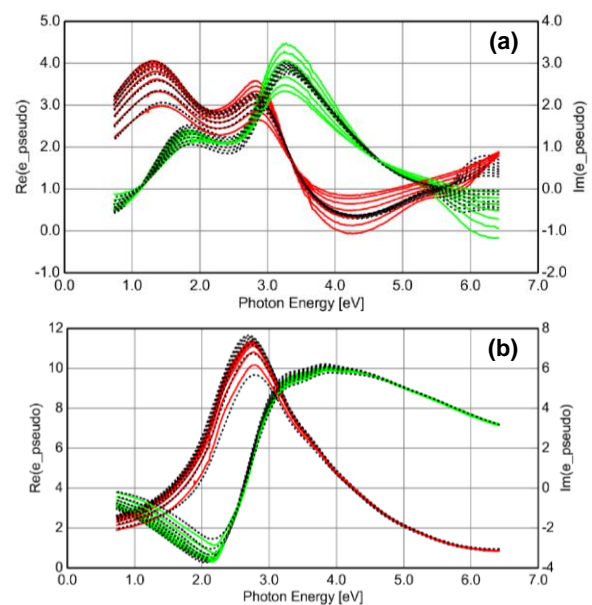


Fig. 4. Ellipsometry data expressed as complex pseudo dielectric function, for sample annealed at (a) 300 °C and (b) 600 °C. The color solid lines are experimental data (red = real part, green = imaginary part), black dashed line fit.

Within this optical model: (i) the thickness of MnFe_2O_4 film was estimated to be 30 nm, as the optical model fails to describe optical properties when thickness is below 20 nm and above 50 nm. However, we have checked that the change of MnFe_2O_4 film thickness does not modify the nature of the determined optical constants, just its strengths (amplitudes). (ii) surface roughness used in the optical model was 8 nm, as determined by AFM (iii) optical properties of glass substrate were determined by independent ellipsometric measurements (data not shown). The dielectric functions of MnFe_2O_4 are shown in **Fig. 5**.

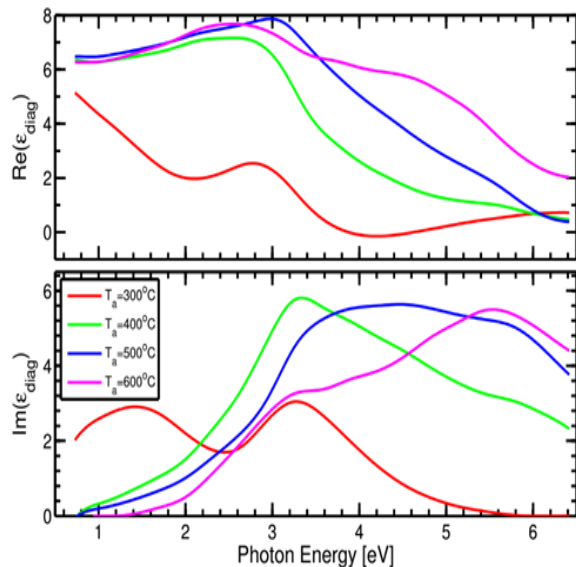


Fig. 5. Real and imaginary part of dielectric functions (i.e. diagonal permittivity) ϵ_{diag} of MnFe_2O_4 ferrites.

The dominant feature for $T_a = 600^\circ\text{C}$ is presence of gap of size 2 eV, demonstrating that the MnFe_2O_4 thin films are semiconducting. This behavior is also kept for lower annealing temperatures 500°C and 400°C , however the quality of gap is decreasing. This has been clearly demonstrated by increase of light absorption (i.e. increase of $\text{Im}(\epsilon)$ in gap area). In case of the smallest annealing temperature $T_a = 300^\circ\text{C}$, the additional absorption peak at 1.5 eV appears and hence this material is not semiconducting. It corresponds to absence of spinel structure, in tune with the XRD analysis of MnFe_2O_4 at 300°C .

Magneto-optical properties of MnFe_2O_4 Thin films: Magneto-optical Kerr effect

The spectral dependencies of the MOKE is shown in **Fig. 6(a)**, where MOKE is expressed by Kerr rotation and Kerr ellipticity. The larger noise of Kerr ellipticity originates from the experimental setup. Using multilayer optical model [32], the off-diagonal permittivity K of MnFe_2O_4 (**Fig. 6(b)**) has been determined; the real part denotes change of light absorption due to magnetization (magnetic dichroism), whereas imaginary part corresponds to

change of the speed of light due to magnetization (magnetic birefringence). The largest off-diagonal permittivity appears in the vicinity of the gap, demonstrating that electronic states near the gap are split by spin-orbit coupling. The largest off-diagonal permittivity appears for $T_a = 400^\circ\text{C}$ and decreases towards higher annealing temperatures. This is in similar with behavior observed for saturation magnetization. It suggests that also complete spinel structure provides reduction of spin-orbit splitting compared to incomplete spinel structure. For the smallest annealing temperature $T_a = 300^\circ\text{C}$, no MOKE effect was observed. It agrees with found very small magnetization, due absence of the spinel structure. Note that found K is about one order smaller compared to PMOKE of 3d-metals, corresponding to small spin-orbit splitting in MnFe_2O_4 , which we attribute to small orbital angular momentum of both Mn and Fe [40].

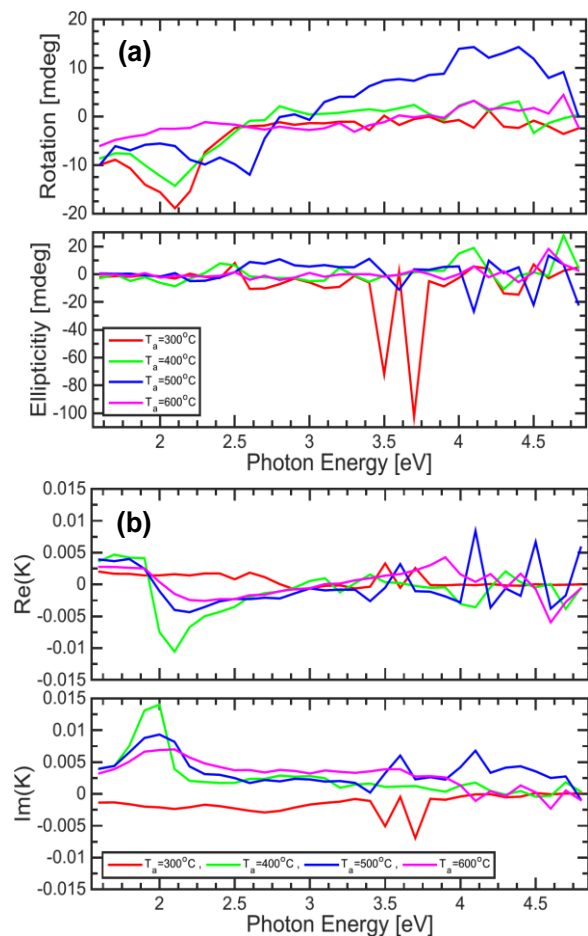


Fig. 6. (a) Polar MOKE spectra of MnFe_2O_4 ferrites. (b) Off-diagonal magneto-optical permittivity (K) of MnFe_2O_4 ferrites.

Conclusion

Homogeneous, smooth, and continuous nanostructured thin films of MnFe_2O_4 were fabricated using chemical approach. Thin films fabricated using chemical approach has demonstrated to be a suitable tool to achieve homogeneous thin films which are

highly transparent. The structural, magnetic, optical and magneto-optical properties of the fabricated thin films have been investigated. Structural analysis of thermally annealed MnFe_2O_4 thin films showed a crystalline phase with spinel structure for the annealing temperature (T_a) of 500 °C and above. Furthermore, as the annealing temperature of the film increases, the intensity of characteristic XRD peaks increased significantly, demonstrating higher quality of crystalline phase of ferrites. The structural transitions have been reflected by the change of optical properties. The size of MnFe_2O_4 particles was observed to be 70-180 nm with ellipsoidal morphology and surface roughness (rms) equals to 8 nm. M-H hysteresis loops indicated that the magnetic properties of MnFe_2O_4 thin films depends on both their nanostructures and the annealing temperatures. Namely, hysteresis loops of the ferrite thin films indicated ferromagnetic behavior for annealing temperatures 400 °C and above. The annealed films showed semiconducting behavior at and above 400 °C annealing temperature. The magneto-optical properties of MnFe_2O_4 thin films indicated that the Kerr rotation is small (i.e., one order less) when compared to CoFe_2O_4 or metallic Fe, Co films, related to small orbital momentum of both Fe and Mn. The as fabricated thin films could be used as magnetic sensors.

Acknowledgements

The authors acknowledge partial support from the project CZ.1.05/1.1.00/02.0070 (IT4Innovations), PostDoc II project opportunity for young researchers Reg.No. CZ.1.07/2.3.00/30.0055 and GACR 13-30397S. The authors acknowledge Robin Silber, Klára Drobíková, Kateřina Mamulová Kutlákova, Lenka Matejová, Ondrej Zivotsky, Vladimír Tomášek for making available the instrumentation facilities. The authors thank Prof. G. Bhagavannarayana, RGUKT, IIIT-RK Valley, Ex-Chief Scientist, NPL, New Delhi, for helping us in improving the manuscript.

Author's contributions

Conceived the plan: Illa Ramakanth; Performed the experiments: Illa Ramakanth, Robin Silber, Klára Drobíková, Kateřina Mamulová Kutlákova, Lenka Matejová, Ondrej Zivotsky, Vladimír Tomášek; Data analysis: Illa Ramakanth; Wrote the paper: Illa Ramakanth. Authors have no competing financial interests.

Supporting information

Supporting information available.

References

- Guo, P.; Cui, L.; Wang, Y.; Lv, M.; Wang, B.; Zhao, X.S.; *Langmuir*, **2013**, *29*, 8997.
- Srikanth, S.; Bliznyuk, V. N.; Binekc, C.; Evgeny, Y.; Symbal, T.; *J. Mater. Chem.*, **2011**, *21*, 16819.
- Aulakh, D.; Pyser, J. B.; Zhang, X.; Yakovenko, A. A.; Dunbar, K. R.; Wriedt, M.; *J. Am. Chem. Soc.*, **2015**, *137*, 9254.
- Jalkanen, P.; Tuboltsev, V.; Marchand, B.; Savin, A.; Puttaswamy, M.; Vehkamäki, M.; Mizohata, K.; Kemell, M.; Hatanpää, T.; Rogozin, V.; Räisänen, J.; Ritala, M.; Leskelä, M.; *J. Phys. Chem. Lett.*, **2014**, *5*, 4319.
- Diodati, S.; Pandolfo, L.; Caneschi, A.; Gialanella, S.; Gross, S.; *Nano Res.*, **2014**, *7*, 1027.
- Kumar, S. S.; Venkateswarlu, P.; Rao, V. R.; Rao, G. N.; *Int. Nano Lett.*, **2015**, *5*, 395.
- Reitz, C.; Suchomski, C.; Chakravadhanula, V. S. K.; Djerdj, I.; Jagličić, Z.; Brezesinski, T.; *Inorg. Chem.*, **2013**, *52*, 3744.
- Šimša, Z.; Thailhades, P.; Presmanes, L.; Bonningue, C.; *J. Magn. Magn. Mater.*, **2002**, *242-245*, 381.
- Comstock, R. L.; *J. Mater. Sci.: Mater. Electron.*, **2002**, *13*, 509.
- Demir, A.; Güner, S.; Bakis, Y.; Esir, S.; Baykal, A.; *J. Inorg. Organomet. Polym. Mater.*, **2014**, *24*, 729.
- Brachwitz, K.; Böntgen, T.; Lorenz, M.; Grundmann, M.; *Appl. Phys. Lett.*, **2013**, *102*, 172104.
- Tirosh, E.; Markovich, G.; *Adv. Mater.*, **2007**, *19*, 2608.
- Liu, X.; Chen, Y.; Wang, L.; Peng, D-L.; *J. Appl. Phys.*, **2013**, *113*, 076102.
- Gu, Y.; Kornev, K. G.; *Part. Part. Syst. Char.*, **2013**, *30*, 958.
- Puntes, V. F.; Krishnan, K. M.; Alivisatos, A. P. *Science*, **2001**, *291*, 2115.
- Lin, X. M.; Samia, A. C. S.; *Synthesis, J. Magn. Magn. Mater.*, **2006**, *305*, 100.
- Fried, T.; Shemer, G.; Markovich, G.; *Adv. Mater.*, **2001**, *13*, 1158.
- Sun, S. H.; Murray, C. B.; *J. Appl. Phys.*, **1999**, *84*, 4325.
- Quickel, T. E.; Le, V. H.; Brezesinski, T.; Tolbert, S. H. *Nano Lett.*, **2010**, *10*, 2982.
- Nakano, M.; Tomohara, K.; Song, J. M.; Fukunaga, H.; *J. Appl. Phys.*, **2000**, *87*, 6217.
- Adam, J. D.; Krishnaswamy, S. V.; Talisa, S. H.; Yoo, K. C.; *J. Magn. Magn. Mater.*, **1990**, *83*, 419.
- Darshanea, S. L.; Suryavanshia, S. S.; Mulla, I. S.; *Ceram. Int.*, **2009**, *35*, 1793.
- Yu, S. H.; Yoshimura, M.; *Chem. Mater.*, **2000**, *12*, 3805.
- Sharma, A.; Afsar, M. N.; *J. Appl. Phys.*, **2011**, *109*, 07A503.
- Marsan, E.; Gauthier, J.; Chaker, M.; Wu, K.; *IEEE Int. Conf. Nano Eng. Mol. Syst.*, **2005**, *3rd*, 279.
- Lee, J. H.; Huh, Y. M.; Jun, Y.W.; Seo, J. W.; Jang, J. T.; Song, H. T.; Kim, S.; Cho, E. J.; Yoon, H. G.; Suh, J. S.; Cheon, J.; *Nat. Med.*, **2006**, *13*, 95.
- Tromsdorf, U. I.; Bigall, N. C.; Kaul, M. G.; Bruns, O. T.; Nikolic, M. S.; Mollwitz, B.; Sperling, R. A.; Reimer, R.; Hohenberg, H.; Parak, W. J.; Förster, S.; Beisiegel, U.; Adam, G.; Weller, H.; *Nano Lett.*, **2007**, *7*, 2422.
- Yang, L. X.; Wang, F.; Meng, Y. F.; Tang, Q. H.; Liu, Z. Q.; *J. Nanomater.*, **2013**, *1*.
- Chen, A.; Hutchby, J.; Jhirnov, V.; Bourianoff, G. (Eds.); *Emerging Nanoelectronic Devices*; Wiley: USA, **2015**.
- Johs, B.; Hale, J. S.; *Phys. Status Solidi A*, **2008**, *205*, 715.
- Rathgen, H.; Katsnelson, M. I.; *Phys. Scr., T.*, **2004**, *109*, 170.
- Visnovsky, S. *Czech. J. Phys. B* **1986**, *36*, 626.
- Price, G. D.; Price, S. L.; Burdett, J. K.; *Phys. Chem. Miner.*, **1982**, *8*, 69.
- Musata, V.; Potecasua, O.; Beleab, R.; Alexandrua, P.; *Mater. Sci. Eng. B.*, **2010**, *167*, 85.
- Takadate, K.; Yamamoto, Y.; Makino, A.; Yamaguchi, T.; Sasada, I.; *J. Appl. Phys.*, **1998**, *83*, 6854.
- Wang, Y. C.; Ding, J.; Yi, J. B.; Liu, B. H.; *Appl. Phys. Lett.*, **2004**, *84*, 2596.
- Tang, Z. X.; Sorensen, C. M.; Klabunde, K. J.; Hadjipanayis, G. C.; *Phys. Rev. Lett.*, **1991**, *67*, 3602.
- Bateer, B.; Tian, C.; Qu, Y.; Du, S.; Yang, Y.; Ren, Z.; Pan, K.; Fu, H.; *Dalton Trans.*, **2014**, *43*, 9885.
- Guo, P.; Zhang, G.; Yu, J.; Li, H.; Zhao, X.S.; *Colloids and Surfaces A: Physicochem. Eng. Aspects*, **2012**, *395*, 168.
- Szotek, Z.; Temmerman, W. M.; Ködderitzsch, D.; Svane, A.; Petit, L.; Winter, H.; *Phys. Rev. B*, **2006**, *74*, 174431.